# Binding Strength of Porphyrin–Gold Nanoparticle Hybrids Based on Number and Type of Linker Moieties and a Simple Method To Calculate Inner Filter Effects of Gold Nanoparticles Usin...

**ARTICLE** *in* THE JOURNAL OF PHYSICAL CHEMISTRY A · JANUARY 2015

Impact Factor: 2.69 · DOI: 10.1021/jp510924n · Source: PubMed



**6 AUTHORS**, INCLUDING:

Tauqir Ali Sherazi
COMSATS Institute of Information Technology
**34** PUBLICATIONS **114** CITATIONS
SEE PROFILE

Zafar Iqbal
COMSATS Institute of Information Technology
**17** PUBLICATIONS **164** CITATIONS
SEE PROFILE

Sohail Anjum Shahzad
Changchun Institute Applied Chemistry
**48** PUBLICATIONS **317** CITATIONS
SEE PROFILE

THE JOURNAL OF PHYSICAL CHEMISTRY A

Article

pubs.acs.org/JPCA

# Binding Strength of Porphyrin–Gold Nanoparticle Hybrids Based on Number and Type of Linker Moieties and a Simple Method To Calculate Inner Filter Effects of Gold Nanoparticles Using Fluorescence Spectroscopy

Ahson J. Shaikh,*[,†,‡] Faiz Rabbani,[†] Tauqir A. Sherazi,[†] Zafar Iqbal,[†] Sadullah Mir,[†] and Sohail A. Shahzad[†]

[†]Department of Chemistry, COMSATS Institute of Information Technology, Abbottabad-22060, Pakistan

[‡]Department of Chemical Engineering, Delft University of Technology, Julianalaan 136, 2628 BL Delft, The Netherlands

Supporting Information

**ABSTRACT:** Gold nanoparticle–porphyrin assemblies were formed by binding functionalized porphyrins to gold nanoparticles (Au-NPs). Spectroscopic properties of hybrids and binding strength of porphyrins to Au-NPs were observed based on number and type of linker moieties using fluorescence spectroscopy. Binding appears to be dependent on number rather than type of linker moieties present on the porphyrin molecules, as tetraaminophenyl porphyrin shows the highest binding among the molecules we studied and causes agglomeration of nanoparticles due to presence of four linker groups. The inner filter effects of Au-NPs are considerably high due to their high extinction coefficient and cause large errors in the evaluation of quenching efficiencies. We have described a very simple method to calculate the inner filter effects of Au-NPs by first loading them with porphyrins and then replacing them with nonfluorescent ligands. The difference in the fluorescence of unbound porphyrins in the presence and absence of Au-NPs describes their inner filter effects.

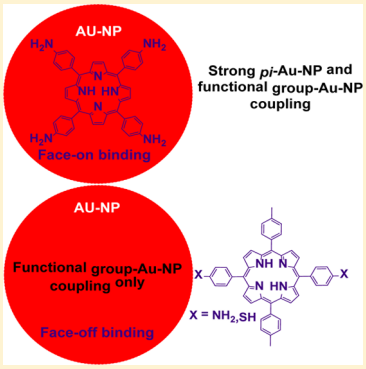


## INTRODUCTION

In continuation to our previous efforts on the influence of the chemical structure on the stability, conductance, and charge transport through porphyrin single-molecule junctions,[1−3] we have also studied binding interaction of synthesized porphyrin molecules to gold nanoparticles in solution based on number and type of linker moieties.[4−8] These studies are crucial to get insight into molecule–nanoparticle interactions, specifically binding affinity and electronic properties of the Au-nanoparticle–porphyrin assemblies.

Porphyrins are chosen for such studies because of their interesting spectroscopic and electronic properties with great architectural flexibility to tune electronic/binding properties by various modifications around the molecule. Porphyrins are complex, highly conjugated aromatic molecules with chemically stable structures and the ability to self-assemble on surfaces as well as in solution.[9−12] Porphyrins are also interesting molecules for their conductivity properties.[13−18]

Gold nanoparticles (Au-NPs) are regularly used in combination with organic molecules, polymers[19,20] and biological molecules[21−24] for various functionalities,[25] where such molecules act as ligands or stabilizing agents for nanoparticles. Using the conductive properties of gold nanoparticles and specifically designed organic molecules, conjugates with new functionalities and properties can be obtained.

There are few examples in literature, where porphyrins are bound to Au-NPs; for example, Teranishi and coworkers[8] reported that Au nanoparticles are protected with the porphyrin rings, parallel to the Au surface, because all iminic nitrogen atoms of porphyrins participate in the ligation to the Au nanoparticle surface. Same authors recently reported[4] face-on and close configuration of a $\pi$-conjugated porphyrin molecule on an Au cluster, generating a strong $\pi$–metal coupling between the $\pi$ and metal orbitals.

The conformation of porphyrin molecules linked to nanoparticles or nanoelectrodes can be described as face-on binding, for example, porphyrin molecule lying flat on the surface of nanoelectrode, and face-off binding, for example, molecule linked via linkers perpendicularly to the surface of nanoparticles or nanoelectrode(s). Such studies have been reported in details using conductance of porphyrin molecules.[2] We used fluorescence spectroscopy as a tool to study binding of porphyrins to Au-NPs by calculating the binding constants using Stern–Volmer plots. When using fluorescence spectroscopy, inner filter effects of Au-NPs interfere with the binding of porphyrins by showing decreased fluorescence. These inner filter effects arise from strong absorption of Au-NPs that

**Received:** October 31, 2014
**Revised:** January 16, 2015
**Published:** January 22, 2015





DOI: 10.1021/jp510924n
J. Phys. Chem. A 2015, 119, 1108−1116

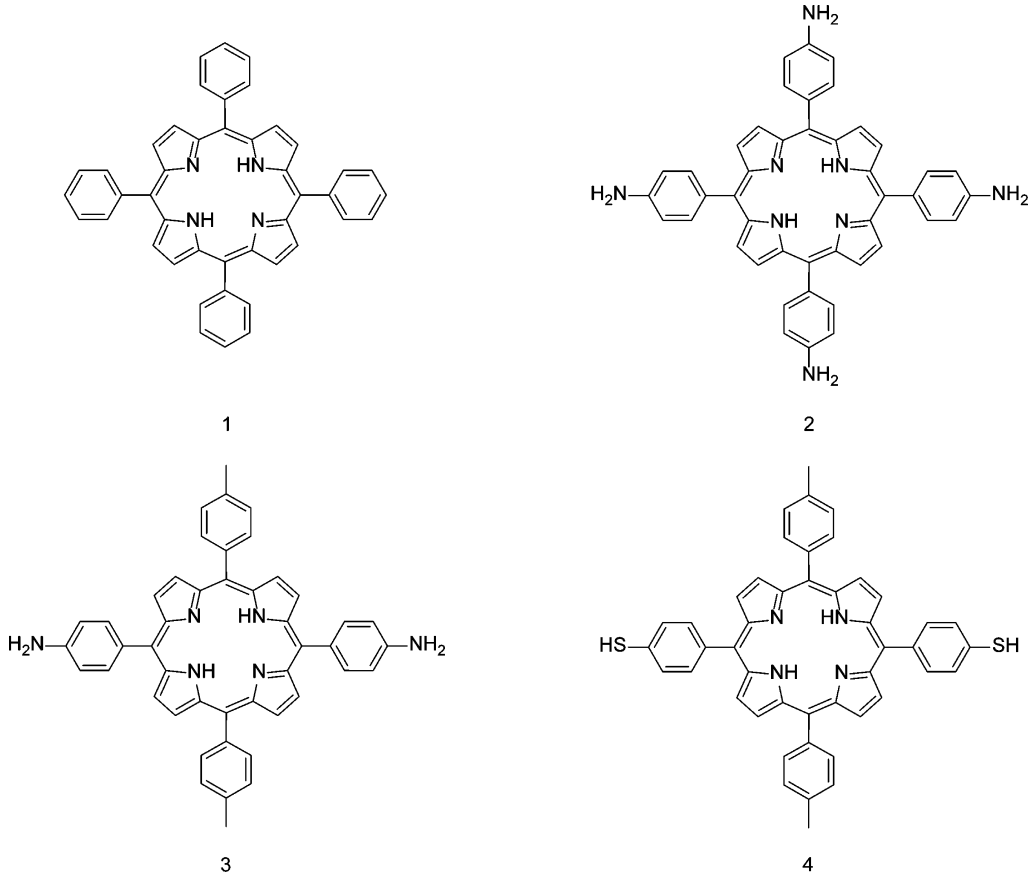


**Figure 1.** Porphyrins used to study their binding with Au-NPs.

overlap with the excitation and emission spectrum of interest, leading to partial absorption of the excitation beam as well as emitted light, which, in turn, results in a decrease in the observed fluorescence intensity. In the situation of porphyrins bound to Au-NPs, the inner filter effects are due to the strong absorption of the Au-NPs and increase with each addition in a titration experiment. Inner filter effects can in part be reduced by using a cuvette with short path-length to avoid excessive absorption of the light but cannot be completely eliminated because of the high extinction coefficient of Au-NPs. These inner filter effects can cause large errors in the evaluation of quenching efficiencies.

## MATERIALS AND METHODS

Porphyrins were synthesized and characterized as described previously.[1−3] Extinction coefficient of porphyrin **2** was calculated to be $2.484 \times 10^5$ L mol$^{-1}$ cm$^{-1}$ by measuring UV−vis absorption at 428 nm of five different dilutions in THF. The lifetime fluorescence decay for porphyrin **2** is 7.35 ns, 7.72 ns for porphyrin **3** and 7.24 ns for porphyrin **4**.

Dodecylamine and other organics/inorganics were available commercially and were used without further purification. All solvents used for reactions were purified with the use of MBRAUN solvent purification system MB SPS-800. Milli-Q-water was used, whenever required for the preparation of gold nanoparticles.

**Synthesis of Au Nanoparticles.** Au-NPs were synthesized in organic phase according to the literature procedures.[26] Synthesis of gold nanoparticles in organic phase was carried out by dissolving 0.75 g dodecylamine in 25 mL of cyclohexane, then 6 mL of aqueous formaldehyde (37%) was added. After vigorous stirring for 10 min at room temperature, the cyclohexane phase was separated and washed twice with water. Next, 10 mL of aqueous $HAuCl_4$ solution (1 g $HAuCl_4$ in 250 mL $H_2O$) was added to the cyclohexane solution under vigorous stirring. Stirring was continued at room temperature for 40 min, and the color of the organic phase turned to deep ruby red, indicating the formation of gold nanoparticles. The aqueous phase was separated, and the organic solution of gold nanoparticles was obtained. The UV−vis absorption spectrum showed a strong band at 515 nm. DLS confirmed that nanoparticles with a diameter of 7.6 ± 0.8 nm (including ligand; vide infra) and actual diameter of 4.4 ± 0.8 nm were formed. Because the diameter of nanoparticles found from UV−vis spectra[27] and DLS measurements was in good agreement with the reported method, we did not measure size using TEM.

The extinction coefficient of Au-NPs was calculated to be $9 \times 10^6$ L mol$^{-1}$ cm$^{-1}$ by measuring UV−vis absorption at 515 nm of five different dilutions in THF.

**UV−vis and Fluorescence Measurements.** UV−vis measurements were performed in AnalytikJena Specord 250 spectrometer equipped with a deuterium lamp and a halogen lamp. Quartz cuvettes were used with path lengths of 10 mm. Fluorescence spectroscopy was performed on a Jasco J-815 CD-spectrometer. The cuvette was quartz with dimensions 3 × 3 mm. For determination of luminescence lifetimes, a LifeSpecs-ps (Edinburgh instruments) was used with excitation pulses of 70 ps at 405 nm.


DOI: 10.1021/jp510924n
J. Phys. Chem. A 2015, 119, 1108−1116

Samples were prepared by combining the correct amounts and appropriate ratios from stock solutions of gold nanoparticles and porphyrins in THF. For fluorescence and UV−vis measurements, the concentration of porphyrins was kept constant at 0.75 $\mu$M. The addition of gold nanoparticles was from 0 to 100 $\mu$L (1 $\mu$M) with difference of 10 $\mu$L for each measurement. Final concentrations were calculated for a solution of 2 mL of each sample. 70 $\mu$L from 2 mL of each prepared sample was used for fluorescence measurements, and the rest was used for UV measurements. Samples were not used twice. In general, the samples were mixed and kept overnight, and next day measurements were recorded.

**Gel Permeation Chromatography.** Gel permeation chromatography (purification and purity-trace) was performed on a Waters Gel Permeation chromatography machine, LC-8A pump with a Waters 2487 dual $\lambda$ absorbance detector. The column used here was the reprogel PS-GPC 500, 5 $\mu$m particle size dimensions 300 × 30 mm for preparative with a 6 mL/min (THF) flow; for analytical measurements, the same column with dimensions 30 × 8 mm was used with a flow of 1 mL/min (THF). Porphyrin-bound gold nanoparticles were separated from free porphyrins by these columns.

**Dynamic Light Scattering.** Dynamic light scattering (DLS) measurements were performed on the Zetasizer Nano ZS from Malvern Instruments Limited using the 173° angle noninvasive backscatter mode and the M3-phase analysis light scattering mode, respectively. The instrument had a red 4.0 mW 633 nm He−Ne laser. The multiple peak high-resolution fitting procedure was used to obtain the particle size distribution from the autocorrelation function. DLS spectra were measured at room temperature in THF. Intensity distribution curves for Au-NPs were considered for particle size distribution. Measurements were performed with nanoparticles at 1 $\mu$M concentration, nanoparticles passed through GPC column, and nanoparticles treated with porphyrin **2** and passed through GPC column.

## RESULTS AND DISCUSSION

**Porphyrins.** The porphyrins used for our binding studies differ in the nature (as amino vs thiol functional groups) and number of gold binding linkers (two vs four) located at their periphery, as shown in Figure 1. Their synthesis has been described elsewhere.[1−3]

**Synthesis of Gold Nanoparticles.** Gold nanoparticles (Au-NPs) were synthesized in organic phase according to the literature procedure.[26] Dodecylamine was initially dissolved in cyclohexane; then, aqueous formaldehyde was added. After vigorously stirring at room temperature, the cyclohexane phase was separated out. Aqueous $HAuCl_4$ solution was added to the separated cyclohexane phase. The color turned to deep ruby red, indicating the formation of gold nanoparticles. The UV−vis absorption spectrum showed a strong band at 515 nm characteristic for a gold plasmon band, indicating that gold nanoparticles with a diameter of ∼4.38 nm were formed.[27] This was confirmed by DLS, which revealed that nanoparticles with a hydrodynamic diameter of 7.6 ± 0.8 nm (including ligand; vide infra) and actual diameter of 4.4 ± 0.8 nm were formed. Because the diameter of nanoparticles found from UV−vis spectra[27] and DLS measurements was in good agreement with the reported method, we did not measure size using TEM.

**Concentration of Gold Nanoparticles.** To find out the binding affinity of porphyrins to a nanoparticle and quantify porphyrin molecules bound to a single gold nanoparticle, we needed to know the concentration of nanoparticles. The extinction coefficient of nanoparticles solution can also be calculated, once the concentration is known. The precursor salt is reduced to nanoparticles solution, where each nanoparticle constitutes the number of gold atoms. If the size of nanoparticles is determined, then by using a standard formula, the number of gold atoms in each particle can be calculated, which leads us to the concentration of gold nanoparticles.

The concentration of gold nanoparticles in solution (organic phase) was determined by the method described by Huo et al.[28] and Guo et al.,[29] using the average Au-NP size. Repeated DLS measurements showed that the average particle consisting of an Au core and a surfactant shell had a hydrodynamic diameter of 7.6 ± 0.8 nm. Assuming a length of 1.6 nm for an extended dodecylamine surfactant molecule, the particles contain an Au core of ∼4.4 ± 0.8 nm. This corresponds to 2650 ± ∼1450 atoms for each nanoparticle, if it is assumed that all of the particles are spherical in shape. Face-centered cubic gold density parameters were used to calculate the number of Au atoms per nanoparticle.[28,30]

On dividing the concentration of total Au atoms with the number of Au atoms present in each nanoparticle, the concentration of Au-NPs can be estimated, assuming that all precursor gold salt has been transformed into nanoparticles. Starting from 5 mM solutions of $AuCl_3{\cdot}3H_2O{\cdot}HCl$, the concentration of gold nanoparticles in the organic phase is estimated to be $1.9 \times 10^{-6}$ M in THF. All fluorescence and UV experiments were carried out with the same nanoparticle solution for accuracy purposes. However, for GPC experiments, a new batch was synthesized, where DLS indicated slightly larger nanoparticles.

**Binding of Porphyrins to Spherical Gold Nanoparticles.** UV−vis spectroscopy, fluorescence spectroscopy (steady state and lifetime measurements), gel permeation chromatography (GPC), and dynamic light scattering (DLS) were used to investigate interaction of porphyrins with gold nanoparticles in our studies.

Initially, UV−vis and fluorescence spectroscopy techniques were used to study binding of porphyrins to Au-NPs because changes in electronic spectra were expected upon the addition of gold nanoparticles because of the electronic interactions between porphyrins and gold nanoparticles. UV−vis spectroscopy can be used to observe any change in size of particles or the agglomeration of particles by monitoring change in the absorption peak of nanoparticles. It was also used to determine the number of porphyrins attached to each nanoparticle (vide infra).

In a first series of experiments, UV−vis spectrophotometric titrations of porphyrins **1**, **2**, **3**, and **4** by Au-NPs were performed. Figure 2 shows a series of UV−vis spectra obtained upon the addition of increasing amounts of Au-NP solution to a solution of porphyrin **4**.

The analysis revealed that the change of the spectra shown in Figure 2 with each aliquot of nanoparticles was due to absorption of gold nanoparticles only. The absorption spectrum of porphyrins was not changed by the addition of Au nanoparticles. Similar results were obtained for porphyrins **1**, **2**, and **3**. The absence of changes in the porphyrin indicates that either the porphyrins did not bind to the Au-NPs or there is only a (very) weak electronic interaction between the porphyrins and the Au-NPs.

Fluorescence spectroscopy was also used to investigate binding of porphyrins to gold nanoparticles because


DOI: 10.1021/jp510924n
J. Phys. Chem. A 2015, 119, 1108−1116

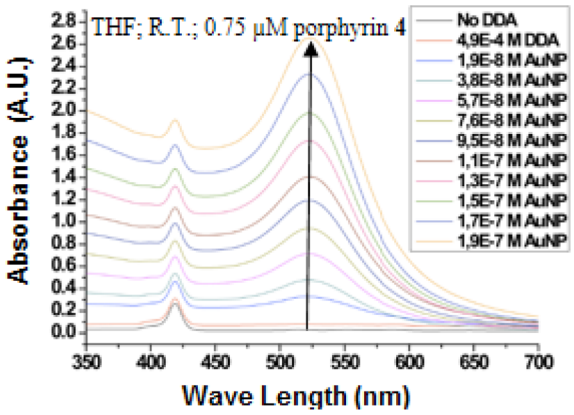


**Figure 2.** UV−vis absorption spectra of porphyrin **4** in THF, which shows that increase in absorption is due to increase in absorption of Au-NPs. The intensity of the porphyrin peak around 420 nm remains the same for all titration measurements, obvious from height of the peak from the baseline for each peak. Dodecyl amine (DDA) effect was minimal as seen from the bottom two spectra with and without DDA present.

fluorescence quenching is usually more sensitive to electronic interactions. The steady-state fluorescence was expected to decrease with each and every addition of Au-NPs, as the porphyrins linked to nanoparticles were expected to transfer their excitation energy to nanoparticles. The steady-state fluorescence studies were complemented by lifetime fluorescence measurement to reveal whether fluorescence quenching is static or dynamic in nature.

Steady-state and lifetime fluorescence spectroscopy techniques were used to study the interaction of gold nanoparticles with various porphyrin molecules. Titrations were carried out with Au-NPs of average size 4.4 nm in THF. The porphyrins were excited at their Soret band (~420 nm), where the extinction coefficient is very high. The Au-NPs have their surface plasmon resonance at ~515 nm. Stern−Volmer plot was calculated as $F_o/F$ versus Au-NP concentration. $F_o$ and $F$ represent the fluorescence intensity of porphyrins before the addition of quencher and after the addition of quencher, respectively, and [Q] represents concentration of quencher, in this case the Au-NPs.

First, as a control the effect of Au-NPs on the fluorescence of tetraphenyl porphyrin (TPP) **1** was studied. Because TPP **1** does not have any groups capable of binding to Au-NPs, strong quenching of the fluorescence was not expected.

Remarkably, the addition of Au-NPs to solution of **1** resulted in a significant decrease in the porphyrin fluorescence (Figure 3a). The Stern−Volmer plot generally represents quenching constant, which in the case of static binding, represents binding constant. The Stern−Volmer plot for TPP (Figure 3b) gives a value of $3 \times 10^6$ $M^{-1}$ as quenching constant. This measurement can be considered as the standard face-on and face-off interaction of porphyrins with gold nanoparticles without any functional group present. Most likely, the observed decrease in fluorescence intensity is partially attributed to inner filter effects of Au-NPs because of their high absorption at ~417 nm (which is also excitation wavelength for porphyrins) and partially due to unspecific binding of TPP to the Au-NP by the interaction with the aliphatic monolayer covering the Au-NPs. Figure 4 shows the effect of nanoparticles on the fluorescence of porphyrin **2**, which has four additional amino groups compared with TPP **1**.

The addition of Au-NPs to solutions of porphyrin **2** also resulted in quenching of its fluorescence, although much stronger than for porphyrin **1**. The quenching can be described by the Stern−Volmer equation, and the Stern−Volmer constant of porphyrin **2** with Au-NPs amounted to $3 \times 10^7$ (Figure 4b). This value is significantly higher than was found for porphyrin **1**, indicating a stronger interaction between **2** and Au-NPs. Time-resolved fluorescence measurements revealed that the fluorescence lifetime was not affected by the addition of Au-NPs, indicating that quenching of the fluorescence of **2** by Au-NPs is a static process, where gold nanoparticles inhibit the excited-state formation by forming a nonfluorescent complex. The lifetime fluorescence decay for porphyrin 2 is 7.35 ns, either free or mixed with Au-NPs. Inner filter effects were kept to a minimum during these measurements by using fluorescence cuvette of 3 mm path length but cannot be excluded completely. As a result, the Stern−Volmer quenching constant is only an approximation of the binding constants of the porphyrin to the Au-NPs. Nevertheless, these measurements reveal that porphyrins with four amino groups have high binding affinity with Au-NPs compared with porphyrin **1** with no amino groups.

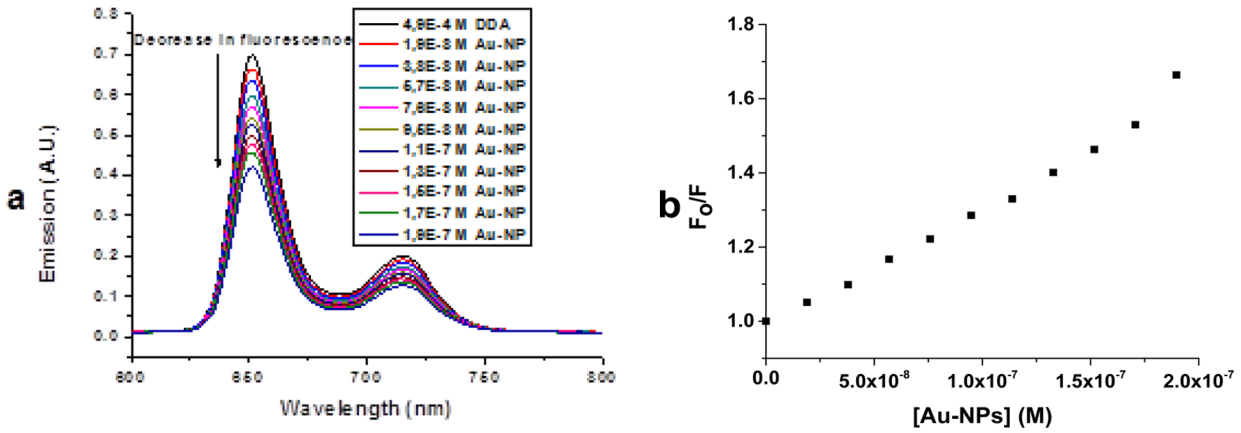


**Figure 3.** (a) Fluorescence quenching of TPP (**1**) by the addition of Au-NPs. Excitation at 417 nm, emission maxima at 651 and 716 nm. (b) Stern−Volmer Plot for TPP (**1**) quenching with Au-NPs shows quenching constant of $3 \times 10^6$ $M^{-1}$. Dodecyl amine (DDA) in porphyrin only solution was added to subtract the (minimal) effects on fluorescence of DDA from Au-NPs solution (vide infra).



DOI: 10.1021/jp510924n
J. Phys. Chem. A 2015, 119, 1108−1116

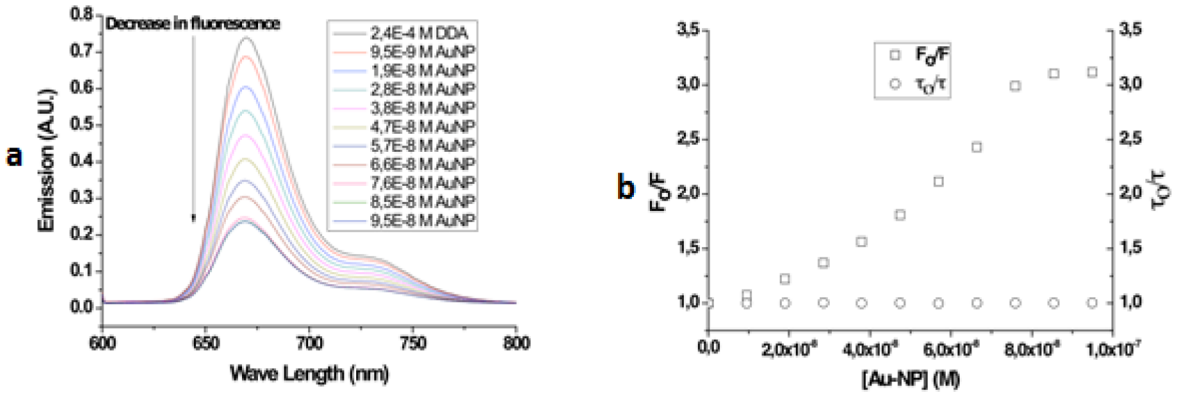


**Figure 4.** (a) Fluorescence quenching of porphyrin **2** when Au-NPs are added and (b) quenching constant (binding constant) of Au-NPs with porphyrin **2** is $3 \times 10^7$ $M^{-1}$, calculated from the Stern–Volmer plot. It also shows lifetime fluorescence measurement of porphyrin **2** (7.35 ns) when mixed with Au-NPs. Dodecyl amine (DDA) in porphyrin-only solution was added to subtract the (minimal) effects on fluorescence of DDA from Au-NPs solution (vide infra).

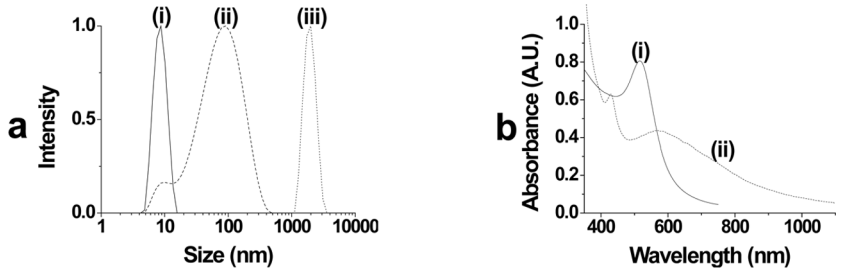


**Figure 5.** (a) Normalized intensity distribution DLS measurements curves for Au-NPs (i) in THF at 1 $\mu$M concentration (—) (ii) passed through GPC column (- - -) (iii) treated with porphyrin **2** and passed through GPC column (....), (b) UV–vis absorption spectrum of Au-NPs before (—) and after treatment (···) with porphyrin **2**. Free porphyrins were separated by GPC.

Because these results clearly indicate that porphyrin **2** with four amino groups binds strongly to Au-NPs, the interaction of porphyrin **3** having two amino groups at trans positions with Au-NPs was also investigated. Also, for this porphyrin the addition of Au-NPs led to quenching of the porphyrin fluorescence (SI; Figure S1a); however, the Stern–Volmer quenching constant amounted to only $4 \times 10^6$ (SI; Figure S1b), indicating that binding of porphyrin **3** with only two amino groups at trans positions is not as strong as that for porphyrin **2** with four amino groups, however slightly higher than porphyrin **1** with no functional groups present.

The lifetime fluorescence measurement (SI; Figure S1b) also shows that it is static quenching rather than dynamic quenching, which confirms that quenching constant is binding constant. The lifetime fluorescence decay for porphyrin **3** is 7.72 ns, either free or mixed with Au-NPs.

Studies with four amino versus two amino groups present in porphyrins reveal that there was much stronger binding for the tetra-amino functionalized porphyrin **2** as compared with the bis-amino functionalized porphyrin **3**. Because thiol functional groups have a higher binding affinity to gold surface as compared with amino groups,[31] it was interesting to study the interaction of thiol-functionalized porphyrins with Au-NPs. The fluorescence quenching of porphyrin **4** results is shown in Figure S2a (SI).

The Stern–Volmer plot for porphyrin **4** (see SI; Figure S2b) did not show significant difference in the quenching constant compared with porphyrin **3**, that is, $3 \times 10^6$. It was nearly similar to porphyrin **3** and TPP (porphyrin **1**), indicating that the presence of two thiol groups at trans positions did not lead to significantly stronger interactions with Au-NPs. The lifetime fluorescence decay for porphyrin **4** is 7.24 ns, either free or mixed with Au-NPs.

The similar binding constants for porphyrins **1**, **3**, and **4** can be explained on the basis of mainly face-off binding of these porphyrins to Au-NPs. The presence of excess dodecylamine molecules as surfactant competes and prevents binding of these porphyrins. In the case of porphyrin **2** with four functional groups present, face-on binding effects are also prominent, which overall increase the binding constant to around one order of magnitude higher as compared with porphyrins **1**, **3**, and **4**.

**DLS and GPC as Complementary Techniques to Study Porphyrins–AuNPs Binding.** The fluorescence quenching studies strongly suggest that porphyrin **2** binds to Au-NPs. Further evidence of binding of porphyrin **2** to Au-NPs was obtained by separation of porphyrins bound to Au-NPs from unbound porphyrin molecules in solution by means of gel permeation chromatography. To this extent, a relatively concentrated 15 mL (~300 $\mu$M) solution of porphyrin **2** in THF was added to 1 mL (1 $\mu$M) of Au-NPs in THF, and the fraction of porphyrins bound to the gold nanoparticles was determined by gel permeation chromatography (GPC) and UV–vis spectroscopy.

The Au-NPs used in these experiments had a hydrodynamic diameter of 8.9 nm, as measured by DLS, before passing them over the GPC column. When a solution of such 8.9 nm Au-NPs was treated with porphyrin **2**, as previously explained, and then passed through GPC column to remove the excess porphyrins, a significant increase in the hydrodynamic diameter of the


DOI: 10.1021/jp510924n
J. Phys. Chem. A 2015, 119, 1108–1116

particles was observed by DLS. The agglomerated size of particles was bigger than 1 $\mu$m, as is clear from the particle size distribution shown in Figure 5a. As a control experiment also Au-NPs without added porphyrin were passed over a GPC column, which, unfortunately, also already caused agglomeration of Au-NPs to clusters with a size of ~100 nm. Most likely, the access of surfactant present (dodecylamine) in the Au-NPs solution was removed through this process, resulting in some agglomeration of the Au-NPs.

Despite this undesired destabilization of Au-NPs, GPC still could be used to separate porphyrins bound to Au-NPs from the free porphyrins in solution. Figure 5b shows the UV−vis absorption spectra of the Au-NPs fractions collected from the preparative GPC column in the absence and presence of porphyrin **2**. The spectrum of the Au-NPs treated with porphyrin **2** shows a clear absorption band with a maximum around 420 nm, characteristic for the Soret band of the porphyrin. This clearly indicates that porphyrin **2** is attached to gold nanoparticles, which is in agreement with the fluorescence measurements previously made. The peak for the Au-NPs has moved from 525 to 570 nm, which is a sign that the size of Au-NPs has increased because of huge aggregation. This enhanced aggregation is due to use concentrated solutions of porphyrins and Au-NPs and removal of surfactants (DDA) by GPC, resulting in larger overall plasmon resonance leading to red shift in the absorption spectrum.

**Estimation of Number of Porphyrins Attached to Single Au-NP.** Estimation of number of porphyrins attached to each Au-NP was the next logical step to get further knowledge of the porphyrin−Au-NPs binding. The extinction coefficient of porphyrin **2** and gold nanoparticles in THF has been determined to be $2.484 \times 10^5$ L mol$^{-1}$ cm$^{-1}$ (at 428 nm) and $9 \times 10^6$ L mol$^{-1}$ cm$^{-1}$ (at 515 nm), respectively.

In total volume of 2 mL, 100 $\mu$L of nanoparticles (1 $\mu$M) and porphyrins **2** (0.75 $\mu$M) was mixed, and a small fraction (100 $\mu$L) of this mixture (Au-NP−porphyrin complex) was separated from unbound porphyrins using an analytical GPC column with a different flow rate as compared with that shown in Figure 5. Because of the small size of Au-NPs and presence of organic phase, centrifuge did not work to separate them from the mixture of free porphyrins.

The UV−vis absorption spectra of the Au-NPs linked with porphyrins are shown in Figure 6a.

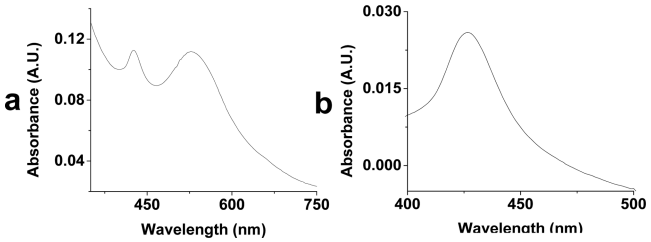


**Figure 6.** (a) UV−vis absorption spectrum for Au-NPs treated with porphyrin **2** and passed through an analytical GPC column. (b) Background corrected for porphyrins.

It was observed that the absorbance maximum associated with the Au-NPs had shifted from 515 to 528 nm, which also points to agglomeration of particles, or in other words, increase in size of Au-NPs[32] due to interaction with porphyrins **2**. The agglomeration effect seen in Figure 6 is small as compared with the agglomeration effect seen in Figure 5b (ii), and the reason is the higher concentration of porphyrins, AU-NPs, and a different flow rate used in the preparative GPC column.

The contribution of porphyrin absorption to the total absorption was obtained by subtracting the nanoparticles absorption. From the absorption of the resulting peak at 427 nm (Figure 6b) it was calculated that the concentration of porphyrins amounts to ~100 nM, whereas the concentration of Au-NPs is 12 to 13 nM, which corresponds to roughly seven to nine porphyrins for each Au-NP. It should be noted that these results should be interpreted with care because distortion of the Au-NPs spectra (Figure 7) due to agglomeration prohibited a reliable deconvolution of the spectra.

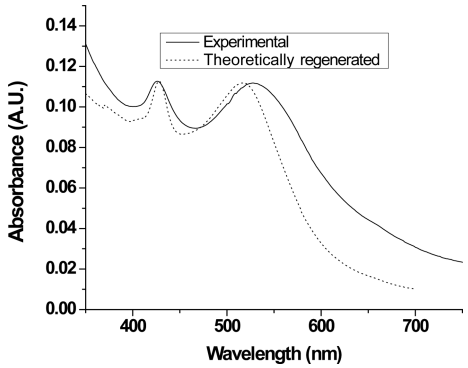


**Figure 7.** UV−vis absorption spectrum for Au-NPs treated with porphyrin **2** and passed through an analytical GPC column (solid line, same as Figure 6a); regeneration of spectrum in Figure 6a by adding individual spectra of porphyrins and gold nanoparticles of known concentrations (dotted line).

As an alternate strategy to calculate number of porphyrins attached to each nanoparticle, we measured UV−vis spectra of porphyrin **2** ($8.25 \times 10^{-7}$ M) and Au-NPs ($8.77 \times 10^{-8}$ M) independently. With various attempts, we were able to regenerate the spectrum in Figure 6a of porphyrin coupled to Au-NPs (Figure 7) by varying weight (a) and weight (b) according to the following scheme.

$$\text{weight (a)} \times \text{porphyrin spectrum} + \text{weight (b)} \times \text{Au-NPs spectrum} = \text{spectrum (Figure 6a)}$$

The weight (a) appeared to be 1/16.525, and weight (b) appeared to be 1/7.225. The concentrations of porphyrin and Au-NPs were calculated according to the following formula.

$$\text{concentration of porphyrins in Figure 6a} = \text{weight (a)} \times \text{concentration of porphyrins only}$$

$$\text{concentration of Au-NPs in Figure 6a} = \text{weight (b)} \times \text{concentration of nanoparticles only}$$

The concentration of porphyrin appeared to be $5 \times 10^{-8}$, and the concentration of Au-NPs appeared to be $1.214 \times 10^{-8}$, which gives a ratio of ~4 porphyrin molecules per nanoparticle.

It can be seen from Figure 7 that the theoretically generated curve is blue shift as compared with the red shift of experimentally generated curve for Au-NPs absorption only. It is due to the fact that the theoretically generated spectrum is only the combination of UV−vis spectra of porphyrins and Au-NPs and does not count the increase in size due to the agglomeration of Au-NPs resulting in a red shift.[32] Therefore,


DOI: 10.1021/jp510924n
J. Phys. Chem. A 2015, 119, 1108−1116

this alternate methodology is only an approximate verification of our previous calculation of seven to nine porphyrins for each nanoparticle.

**Inner Filter Effects of Au-NPs.** It was clear from UV−vis and fluorescence spectra that there were considerable inner filter effects during these measurements. Inner filter effects were minimized by using cuvette of 3 mm path length in all of our measurements. We needed to know the extent of inner filter effects of these nanoparticles on fluorescence measurements because they heavily influence the calculation of binding constants.

It should be noted that the systems described so far also contain surfactant molecules as a stabilizer for the Au-NPs, which have to be replaced in part upon binding of the porphyrin. It is known that dye molecules attached to gold nanoparticles can also be replaced by the addition of surfactant molecules, resulting in an increase of fluorescence as more dye molecules are liberated from the nanoparticles.[33] It appeared to us that this feature can be exploited to discriminate between fluorescence intensity decrease due to inner filter effects and due to binding, by performing a competitive displacement experiment with an electronically nonabsorbing surfactant while keeping the porphyrin and Au-NPs concentrations responsible for the strong absorption and eventual inner filter effects constant. Hence, we carried out such a surfactant displacement experiment with porphyrin **2**, which has the highest binding of the four porphyrins used in our studies, in combination with the gold nanoparticles observed via fluorescence quenching studies. These studies were performed in THF as solvent. With the fluorescence quenching studies of porphyrin **2** (Figure 4), it is clear that at a certain concentration of porphyrins and gold nanoparticles there is no further fluorescence quenching observed any more. Further addition of gold nanoparticles only results in further inner filter effects and no binding.

Because these concentrations were known already, the simple strategy we used was to treat the porphyrins ($7.5 \times 10^{-7}$ M) with gold nanoparticles with the highest concentration ($9.5 \times 10^{-8}$ M) obtained from fluorescence quenching studies. The fluorescence of porphyrin only can be seen in Figure 8, curve A. Dodecylamine does not fluoresce, nor is it responsible for inner filter effects; however, the addition of DDA to a solution of **2** resulted in only a minor (5%) increase in the fluorescence of **2** (Figure 8, curve B), probably due to deprotonation of any residual protonated amines in **2**. For other porphyrins (e.g., TPP), the addition of dodecylamine did not lead to an increase or decrease in the fluorescence levels. Because the effect is only minor and specific for **2**, we did not further investigate the cause of increase in fluorescence of porphyrin **2** upon the addition of DDA.

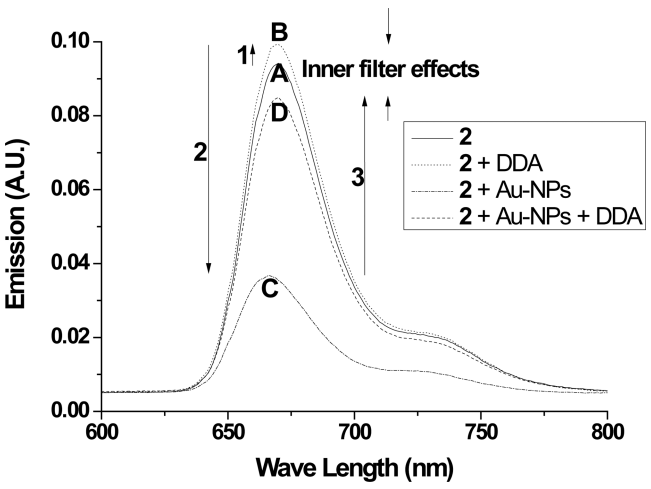


**Figure 8.** Effect of DDA, Au-NPs, and inner filter effects on the fluorescence of porphyrin **2**.

The addition of gold nanoparticles ($9.5 \times 10^{-8}$ M) to a $7.5 \times 10^{-7}$ M solution of porphyrin **2** resulted in an immediate quenching of the porphyrin fluorescence (Figure 8, curve C). However, the addition of DDA liberates porphyrins from the Au-NPs leading to a (partial) restoration of the fluorescence (Figure 8, curve D). In this stage there is no interaction of porphyrins with gold nanoparticles and only inner filter effects are visible. The contribution of inner filter effects can now be determined from the difference in fluorescence intensity between curve B compared with the total maximal quenching (curve C). From the intensities in Figure 8 it was deduced that the total inner filter effects contribute up to 23% of total quenching, whereas 77% of the fluorescence decrease in **2** upon the addition of Au-NPs is due to binding of porphyrin molecules to gold nanoparticles. These values will be influenced by the amount of gold nanoparticles added because of the change in inner filter effects; that is, the higher concentration of nanoparticles shows higher inner filter effects and vice versa. Therefore, each experiment with varied concentration (and size) of Au-NPs needs separate measurements of inner filter effects as size and concentration play an important role in the absorbance of Au-NPs. The binding of porphyrins **1**, **3**, and **4** is relatively weak compared with binding of porphyrin **2**; therefore, the contribution of inner filter effects for porphyrins **1**, **3**, and **4** to the total quenching was not further investigated.

## CONCLUSIONS

We used UV−vis and fluorescence spectroscopy titration experiments to find the binding strength of gold nanoparticle−porphyrin assemblies based on number and type of linker moieties. UV−vis titration experiments showed that the addition of gold nanoparticles does not affect the absorption of porphyrins. Fluorescence studies revealed that binding is dependent on the number rather than type of linker moieties present on the porphyrin molecules. While the diamino porphyrins and dithiol porphyrins show similar binding constants, porphyrins with four amino functionalities (porphyrin **2**) have the highest binding interaction with gold nanoparticles, which was an order of magnitude higher as compared with other porphyrins we used. The presence of four linkers in porphyrin molecule is responsible for additional face-on binding in addition to face-off binding, as compared with other porphyrins. Thiol and amino groups containing porphyrins showing similar binding to the Au-NPs are possibly due to the presence of excess dodecylamine molecule as surfactants, preventing binding of porphyrins to Au-NPs.

The increase in Stern−Volmer plot for all porphyrins is partly due to the inner filter effects of gold nanoparticles, confirmed by UV−vis absorption spectroscopy of the same solutions. The lifetime fluorescence measurement revealed that the binding is static rather than dynamic by showing similar decay constant for porphyrins before and after the addition of nanoparticles. Porphyrin **2** (tetraaminophenyl porphyrin) induces nonselective and uncontrolled binding of gold nanoparticles, leading to agglomeration of Au-NPs, as was observed by DLS measurements. It was due to the presence of


DOI: 10.1021/jp510924n
J. Phys. Chem. A 2015, 119, 1108−1116

four linker groups present in the molecule. The number of porphyrins attached to each gold nanoparticle was calculated to be seven to nine porphyrins/NP using a combination of gel permeation chromatography and UV−vis absorption spectroscopy, and we compared it with theoretically generated spectra, which showed around four porphyrins/NP, which does not count the increase in size due to the agglomeration of Au-NPs resulting in the red shift and is only approximate verification of our calculation of seven to nine porphyrins for each nanoparticle. Other established factors that porphyrin molecules can form stable bridging molecular junctions even without anchoring groups and by adding anchoring groups to the porphyrin backbone increases the stability of the junctions,[2] which also applies to Au-nanoparticles, as observed in the case of porphyrin **1** with no functional group present, still showing some binding to Au-NPs.

The inner filter effects of Au-NPs are considerably high due to the high extinction coefficient of Au-NPs. We have described a very simple method to calculate the inner filter effects of Au-NPs by first loading them with porphyrins and then replacing these porphyrins with nonfluorescent ligand which in this case is dodecyl amine (DDA). The same surfactant molecules (DDA) were acting as stabilizer for the Au-NPs initially, which were first replaced in part upon binding of the porphyrins to Au-NPs, resulting in a decrease in fluorescence. Upon release of porphyrins when DDA was added to the solution, fluorescence increases. This feature was exploited to discriminate between fluorescence intensity decrease due to inner filter effects and due to binding by performing a competitive displacement experiment. The porphyrins and Au-NPs concentrations responsible for the strong absorption and eventual inner filter effects were kept constant. The total inner filter effects contribute up to 23% of total quenching, whereas 77% of the fluorescence decrease upon the addition of Au-NPs is due to binding of porphyrin molecules to gold nanoparticles. These values will be influenced by the amount of gold nanoparticles added because of the change in inner filter effects; that is, the higher concentration of nanoparticles shows higher inner filter effects and vice versa.

These preliminary studies increase our understanding of the binding strength of organic molecules, specifically functionalized porphyrins to Au-NPs. Fluorescence molecules and fluorescence spectroscopy can be used to find inner filter effects of various nanoparticles given the condition that fluorescence molecules bind and unbind to nanoparticles.

## ■ ASSOCIATED CONTENT

### Supporting Information

Fluorescence quenching spectra and Stern−Volmer plot for quenching constant and lifetime fluorescence measurements of porphyrin **3** and **4**. This material is available free of charge via the Internet at http://pubs.acs.org.

## ■ AUTHOR INFORMATION

### Corresponding Author

*E-mail: ahsonjabbar@hotmail.com; ahson@ciit.net.pk. Tel: +92-(0)334-377-0104. Fax: +92-(0)992-383441.

### Notes

The authors declare no competing financial interest.

## ■ ACKNOWLEDGMENTS

A.J.S. is grateful to the Department of Chemical Engineering, Delft University of Technology, Stratingh Institute for Chemistry and the Zernike Institute for Advanced Materials, University of Groningen, The Netherlands for funding.

## ■ REFERENCES

(1) Perrin, M. L.; Martin, C. A.; Prins, F.; Shaikh, A. J.; Eelkema, R.; van Esch, J. H.; van Ruitenbeek, J. M.; van der Zant, H. S. J.; Dulić, D. Charge Transport in a Zinc−Porphyrin Single-Molecule Junction. *Beilstein J. Nanotechnol.* **2011**, *2*, 714−719.

(2) Perrin, M. L.; Prins, F.; Martin, C. A.; Shaikh, A. J.; Eelkema, R.; van Esch, J. H.; Briza, T.; Kaplanek, R.; Kral, V.; van Ruitenbeek, J. M.; et al. Influence of the Chemical Structure on the Stability and Conductance of Porphyrin Single-Molecule Junctions. *Angew. Chem., Int. Ed.* **2011**, *50*, 11223−11226.

(3) Perrin, M. L.; Verzijl, C. J. O.; Martin, C. A.; Shaikh, A. J.; Eelkema, R.; van EschJan, H.; van Ruitenbeek, J. M.; Thijssen, J. M.; van der Zant, H. S. J.; Dulic, D. Large Tunable Image-Charge Effects in Single-Molecule Junctions. *Nat. Nanotechnol.* **2013**, *8*, 282−287.

(4) Tanaka, D.; Inuta, Y.; Sakamoto, M.; Furube, A.; Haruta, M.; So, Y.-G.; Kimoto, K.; Hamada, I.; Teranishi, T. Strongest [Small Pi]-Metal Orbital Coupling in a Porphyrin/Gold Cluster System. *Chem. Sci.* **2014**, *5*, 2007−2010.

(5) Muthukumar, P.; Abraham John, S. Gold Nanoparticles Decorated on Cobalt Porphyrin-Modified Glassy Carbon Electrode for the Sensitive Determination of Nitrite Ion. *J. Colloid Interface Sci.* **2014**, *421*, 78−84.

(6) Gryko, D. T.; Clausen, C.; Lindsey, J. S. Thiol-Derivatized Porphyrins for Attachment to Electroactive Surfaces. *J. Org. Chem.* **1999**, *64*, 8635−8647.

(7) Cormode, D. P.; Davis, J. J.; Beer, P. D. Anion Sensing Porphyrin Functionalized Nanoparticles. *J. Inorg. Organomet. Polym.* **2008**, *18*, 32−40.

(8) Kanehara, M.; Takahashi, H.; Teranishi, T. Gold(0) Porphyrins on Gold Nanoparticles. *Angew. Chem., Int. Ed.* **2008**, *47*, 307−310.

(9) Anderson, H. L. Building Molecular Wires from the Colours of Life: Conjugated Porphyrin Oligomers. *Chem. Commun.* **1999**, 2323−2330.

(10) Noguchi, Y.; Nagase, T.; Ueda, R.; Kamikado, T.; Kubota, T.; Mashiko, S. Fowler-Nordheim Tunneling in Electromigrated Break Junctions with Porphyrin Molecules. *Jpn. J. Appl. Phys., Part 1* **2007**, *46*, 2683−2686.

(11) Kang, B. K.; Aratani, N.; Lim, J. K.; Kim, D.; Osuka, A.; Yoo, K. H. Length and Temperature Dependence of Electrical Conduction through Dithiolated Porphyrin Arrays. *Chem. Phys. Lett.* **2005**, *412*, 303−306.

(12) Sedghi, G.; Sawada, K.; Esdaile, L. J.; Hoffmann, M.; Anderson, H. L.; Bethell, D.; Haiss, W.; Higgins, S. J.; Nichols, R. J. Single Molecule Conductance of Porphyrin Wires with Ultralow Attenuation. *J. Am. Chem. Soc.* **2008**, *130*, 8582−8583.

(13) Qi, P.; Li, Z. H.; Zhou, Y.; Wang, F.; Du, Y.; Zhang, L. Q.; Li, G.; Zhang, H. Z. The Charge Transfer Characteristic of Porphyrin Langmuir−Blodgett Films. *Appl. Surf. Sci.* **2013**, *279*, 349−352.

(14) Beggan, J. P.; Krasnikov, S. A.; Sergeeva, N. N.; Senge, M. O.; Cafolla, A. A. Control of the Axial Coordination of a Surface-Confined Manganese(Iii) Porphyrin Complex. *Nanotechnology* **2012**, *23*, 235606.

(15) Jens, B.; Mathieu, L.; Stefan, K.; Jörg, S.; Alessandro, S.; Shih-Hsin, C.; Germar, H.; Roland, W.; Roy, L.; Paul, H. J. K.; et al. Dynamics of Molecular Self-Ordering in Tetraphenyl Porphyrin Monolayers on Metallic Substrates. *Nanotechnology* **2009**, *20*, 275602.

(16) Qian, G.; Saha, S.; Lewis, K. M. Two-State Conductance in Single Zn Porphyrin Molecular Junctions. *Appl. Phys. Lett.* **2010**, *96*, 243107−3.

(17) Sedghi, G.; Esdaile, L. J.; Anderson, H. L.; Martin, S.; Bethell, D.; Higgins, S. J.; Nichols, R. J. Comparison of the Conductance of Three Types of Porphyrin-Based Molecular Wires: B,Meso,B-Fused



DOI: 10.1021/jp510924n
J. Phys. Chem. A 2015, 119, 1108−1116

Tapes, Meso-Butadiyne-Linked and Twisted Meso-Meso Linked Oligomers. *Adv. Mater.* **2012**, *24*, 653−657.
(18) Welack, S.; Maddox, J. B.; Esposito, M.; Harbola, U.; Mukamel, S. Single-Electron Counting Spectroscopy: Simulation Study of Porphyrin in a Molecular Junction. *Nano Lett.* **2008**, *8*, 1137−1141.
(19) Baker, C. O.; Shedd, B.; Tseng, R. J.; Martinez-Morales, A. A.; Ozkan, C. S.; Ozkan, M.; Yang, Y.; Kaner, R. B. Size Control of Gold Nanoparticles Grown on Polyaniline Nanofibers for Bistable Memory Devices. *ACS Nano* **2011**, *5*, 3469−3474.
(20) Tang, J.; Skotadis, E.; Stathopoulos, S.; Roussi, V.; Tsouti, V.; Tsoukalas, D. Phema Functionalization of Gold Nanoparticles for Vapor Sensing: Chemi-Resistance, Chemi-Capacitance and Chemi-Impedance. *Sens. Actuators, B* **2012**, *170*, 129−136.
(21) Huschka, R.; Zuloaga, J.; Knight, M. W.; Brown, L. V.; Nordlander, P.; Halas, N. J. Light-Induced Release of DNA from Gold Nanoparticles: Nanoshells and Nanorods. *J. Am. Chem. Soc.* **2011**, *133*, 12247−12255.
(22) Guo, X.; Liang, B.; Jian, J.; Zhang, Y.; Ye, X. Glucose Biosensor Based on a Platinum Electrode Modified with Rhodium Nanoparticles and with Glucose Oxidase Immobilized on Gold Nanoparticles. *Microchim. Acta.* **2014**, *181*, 519−525.
(23) Zhang, C.; Li, X.; Tian, C.; Yu, G.; Li, Y.; Jiang, W.; Mao, C. DNA Nanocages Swallow Gold Nanoparticles (Aunps) to Form Aunp@DNA Cage Core−Shell Structures. *ACS Nano* **2014**, *8*, 1130−1135.
(24) Kuzyk, A.; Schreiber, R.; Fan, Z.; Pardatscher, G.; Roller, E.-M.; Hogele, A.; Simmel, F. C.; Govorov, A. O.; Liedl, T. DNA-Based Self-Assembly of Chiral Plasmonic Nanostructures with Tailored Optical Response. *Nature* **2012**, *483*, 311−314.
(25) Pissuwan, D.; Niidome, T.; Cortie, M. B. The Forthcoming Applications of Gold Nanoparticles in Drug and Gene Delivery Systems. *J. Controlled Release* **2011**, *149*, 65−71.
(26) Chen, Y. Y.; Wang, X. K. Novel Phase-Transfer Preparation of Monodisperse Silver and Gold Nanoparticles at Room Temperature. *Mater. Lett.* **2008**, *62*, 2215−2218.
(27) Haiss, W.; Thanh, N. T. K.; Aveyard, J.; Fernig, D. G. Determination of Size and Concentration of Gold Nanoparticles from Uv−Vis Spectra. *Anal. Chem.* **2007**, *79*, 4215−4221.
(28) Liu, X. O.; Atwater, M.; Wang, J. H.; Huo, Q. Extinction Coefficient of Gold Nanoparticles with Different Sizes and Different Capping Ligands. *Colloids Surf., B* **2007**, *58*, 3−7.
(29) Ding, Y. H.; Chen, Z. Q.; Xie, J.; Guo, R. Comparative Studies on Adsorption Behavior of Thionine on Gold Nanoparticles with Different Sizes. *J. Colloid Interface Sci.* **2008**, *327*, 243−250.
(30) Mucic, R. C.; Storhoff, J. J.; Mirkin, C. A.; Letsinger, R. L. DNA-Directed Synthesis of Binary Nanoparticle Network Materials. *J. Am. Chem. Soc.* **1998**, *120*, 12674−12675.
(31) Nath, S.; Jana, S.; Pradhan, M.; Pal, T. Ligand-Stabilized Metal Nanoparticles in Organic Solvent. *J. Colloid Interface Sci.* **2010**, *341*, 333−352.
(32) Amendola, V.; Meneghetti, M. Size Evaluation of Gold Nanoparticles by Uv−Vis Spectroscopy. *J. Phys. Chem. C* **2009**, *113*, 4277−4285.
(33) Nerambourg, N.; Wuerts; Charlot, M.; Blanchard-Desce, M. Quenching of Molecular Fluorescence on the Surface of Monolayer-Protected Gold Nanoparticles Investigated Using Place Exchange Equilibria. *Langmuir* **2007**, *23*, 5563−5570.


DOI: 10.1021/jp510924n
*J. Phys. Chem. A* 2015, 119, 1108−1116